Published in final edited form as:
Cancer Res. 2008 August 15; 68(16): 6822–6830. doi:10.1158/0008-5472.CAN-08-1332.

Stage Specific Inhibitory Effects and Associated Mechanisms of Silibinin on Tumor Progression and Metastasis in TRAMP Model

Komal Raina[1], **Subapriya Rajamanickam**[1], **Rana P. Singh**[1,2], **Gagan Deep**[1], **Manesh Chittezhath**[1], and **Rajesh Agarwal**[1,3]

1*Department of Pharmaceutical Sciences, School of Pharmacy, University of Colorado Denver, Denver, Colorado, USA*

2*Cancer Biology Laboratory, School of Life Sciences, Jawaharlal Nehru University, New Delhi, India*

3*University of Colorado Cancer Center, University of Colorado Denver, Denver, Colorado, USA*

Abstract

Herein, employing transgenic adenocarcinoma of the mouse prostate (TRAMP) model, we assessed the 'stage specific' efficacy of silibinin feeding against prostate cancer (PCa) initiation, progression, angiogenesis and metastasis, and associated molecular events involved in silibinin effects during these stages. Male TRAMP mice starting at 4, 12, 20 and 30 weeks of age were fed with control or 1% silibinin-supplemented diet for 8-15 weeks in stage-specific manners. At the end of studies, silibinin-fed mice showed less severe prostatic lesions compared to positive controls. During early stages of prostate tumor development, silibinin mediated its efficacy mostly *via* anti-proliferative mechanisms. Feeding of silibinin to animals burdened with higher stages of prostate tumor significantly decreased tumor grade *via* anti-proliferative effect, and inhibition of angiogenesis as evidenced by decreased expressions of platelet endothelial cell adhesion molecule-1 (PECAM-1/CD-31), vascular endothelial growth factor (VEGF) and associated receptor, VEGF-R2, hypoxia-inducible factor-1α (HIF-1α) and inducible nitric oxide synthase (iNOS). Metastasis to distant organs was decreased in silibinin-fed mice, which was associated with a decreased expression of matrix metalloproteinases (MMPs), mesenchymal markers snail-1 and fibronectin in the prostatic tissue and retention of epithelial characteristics. Together, these findings are both novel and highly significant in establishing the dual efficacy of silibinin where it inhibits progression of primary prostatic tumor and also shows protective efficacy against angiogenesis and late stage metastasis. These effects of silibinin could have potential implications to improve the morbidity and survival in PCa patients.

Keywords

TRAMP; silibinin; prostate cancer progression; angiogenesis; metastasis; epithelial-mesenchymal transition

Introduction

Prostate cancer (PCa) is the most frequently diagnosed malignancy and leading cause of cancer-related deaths in elderly men (1). One strategy to control this malignancy is its prevention by natural and/or synthetic agents (2-5). In recent years, transgenic adenocarcinoma of the mouse

Requests for reprints: Rajesh Agarwal, Department of Pharmaceutical Sciences, School of Pharmacy, University of Colorado Denver, 4200 East Ninth Street, Box C238, Denver, CO 80262. Phone: (303) 315-1381, Fax: (303) 315-6281, E-mail: Rajesh.Agarwal@uchsc.edu.

prostate (TRAMP) is the most frequently employed animal model to evaluate PCa chemopreventive efficacy of various agents (6-8). TRAMP mice mimic the progressive forms of human PCa; the prostatic histopathology associated with the progression of disease in this model is well characterized and provides a unique opportunity to assess stage specific preventive efficacy of an agent against PCa (9-12). TRAMP mice develop spontaneous progressive stages of prostatic disease (driven by the expression of SV-40 early genes (T/t; Tag) specifically in prostatic epithelium) with time from early lesions of PIN to late stage metastatic adenocarcinoma (11,13,14). We recently reported a dose-dependent inhibitory effect of silibinin (flavonolignan isolated from the seeds of milk thistle) on PCa growth and progression in TRAMP mice, where out of all the doses (0.1-1% w/w), 1% silibinin was most effective, and its anti-PCa effects were neither associated with any adverse effects nor related to suppression of Tag expression (15). Regarding practical and translational aspects, the limitation of this study was that silibinin feeding regimen started at a very early stage when there was no pathological evidence of PCa and continued throughout the experiment (4-24 weeks of age). This makes it impractical to extrapolate the findings of such study to clinical condition where PCa would have been diagnosed in some pathological stage. The clinical usefulness of several chemopreventive agents has similar limitations, due to their suggested daily intake as a preventive measure long before there are any clinical signs of cancerous lesions. An effective alternative to increase the clinical applications of these agents would be to test their efficacy at every stage in tumor development including cancer progression and metastasis. Once it is established that an agent inhibits different stages of malignancy, it would broaden the clinical applications of that agent as well as provide sufficient scientific rationale justifying its recommendation to a patient with clinical signs of cancerous lesions.

Accordingly, the objective of the present study was to assess the stage-specific PCa chemopreventive efficacy of silibinin exploiting the usefulness of TRAMP model where each stage is well-characterized and defined (9-12). We fed 1% silibinin in diet to TRAMP mice at different stages of tumor growth and progression and then determined the efficacy on tumor growth and progression, angiogenesis and metastasis, and elucidated the molecular events involved in silibinin effects.

Materials and Methods

Animals, Treatment and Necropsy

Heterozygous TRAMP (C57BL/6) females were cross-bred with non-transgenic C57BL/6 males, and tail DNA was subjected to PCR-based screening for PB-Tag (14). Routinely obtained TRAMP males (n=15-22 mice/group) were distributed into positive and treatment groups, and starting at 4, 12, 20 or 30 weeks of age were fed with control or 1% silibinin-supplemented [1% silibinin (w/w) in AIN-93M purified] diet and then sacrificed at 12, 20, 30 or 45 weeks of age, respectively (Fig.1). Hereafter, different groups depending upon their study period are referred as 4-12, 12-20, 20-30 and 30-45 week groups, respectively. As overall controls, age-matched non-transgenic mice (n=5 mice/group) were fed control or 1% silibinin diet for same duration. All diets were prepared commercially (Dyets Inc., Bethlehem, PA). Animals were permitted free access to food and water. Food consumption and animal body weight were recorded weekly, and animals monitored daily for general health. Animal care and treatments were in accordance with Institutional guidelines and approved protocol.

During necropsy, each mouse was weighed and lower urogenital tract (LUT) including bladder, seminal vesicles and prostate, was removed *en bloc*. LUT wet weight was recorded, and prostate gland harvested and microdissected wherever possible (when tumor obscured boundaries of lobes, it was taken as such). One portion of dorsolateral prostate was snap-frozen and stored at −80°C. All animals were examined for gross pathology; any evidence of edema, abnormal organ size or appearance in non-target organs was also noted. To ascertain

microscopic pathology, these organs including lung, liver and kidney were also harvested. Tissues were fixed and processed conventionally.

Immunohistochemical (IHC) Analysis

Paraffin-embedded sections (5μ m thick) were deparaffinized and stained using specific primary antibodies followed by DAB staining, as previously described (16). Primary antibodies used were against PCNA (Dako); PECAM-1/CD-31, VEGF (Santa Cruz Biotechnology); SV40 large T antigen (BD Pharmingen); HIF-1α (Novartis) and iNOS (Abcam). Biotinylated secondary antibodies used were rabbit anti-mouse IgG (Dako), goat anti-rabbit IgG and rabbit anti-goat IgG (Santa Cruz Biotechnology). Apoptotic cells were identified by TUNEL (terminal deoxynucleotidyl transferase-mediated dUTP nick end labeling) staining using Dead End Colorometric TUNEL System (Promega Corp.). Positive cells were quantified by counting brown-stained cells among total number of cells at 5 randomly selected fields at ×40 magnification. Immunoreactivity (represented by intensity of brown staining) was scored as 0 (no staining), +1 (very weak), +2 (weak), +3 (moderate) and +4 (strong). For immunofluorescence (IF) analyses, tissue sections were double stained with anti-mouse E-cadherin and anti-rabbit snail-1. Secondary antibodies used were Texas Red goat anti-rabbit IgG and Alexa fluor 488 rabbit anti-mouse IgG (Molecular Probes). Sections were mounted using Vectashield mounting reagent (H-1200) containing DAPI (Vector Labs).

Western Blot (WB) Analysis

Dorsolateral prostate samples were analyzed by immunobloting (17) employing primary antibodies against Cdk2, 4, 6, Cdc2 , Cyclin A, B1, VEGF, VEGF-R1, VEGF-R2, MMP-2, 3, TIMP-2, E-cadherin, uPAR, Fibronectin (Santa Cruz Biotechnology); Cyclin E, Kip1/p27 (Neomarkers); Cip1/p21 (Upstate); HIF-1α (Novartis); iNOS, snail-1 (Abcam); and MMP-9 (Cell Signaling). Secondary antibodies were anti-rabbit IgG (Cell Signaling), anti-mouse IgG (Amersham) and anti-goat IgG (Santa Cruz Biotechnology). Equal protein loading was confirmed by re-probing membranes with β-actin antibody (Sigma).

Statistical and Microscopic Analyses

All statistical analyses were carried out with Sigma Stat software version 2.03 (Jandel Scientific, San Rafael, CA) and two sided P values <0.05 were considered significant. Fisher's Exact test was used to compare incidence of PIN, adenocarcinoma and metastatic lesions, and unpaired two-tailed Student's t-test was employed for all other data. Difference between positive control groups was determined by one-way ANOVA followed by Tukey-test for multiple comparisons. Densitometric analysis of immunoblots (adjusted with β-actin loading control) was by Scion Image program (NIH, Bethesda, MD), and results are reported based on relative densities compared to 4-12 week positive control group. Since control and treated samples were run separately, for comparative densitometric analysis of different immunoblots for the same protein, a correction factor was employed by loading two control samples along with treatment samples to correct differences in density due to experimental variations. All microscopic analyses were done by Zeiss Axioscope 2 microscope (Carl Zeiss, Inc., Jena, Germany) and photomicrographs captured by AxioCam MrC5 camera (Carl Zeiss). All IF analyses were done by Nikon D Eclipse C1confocal microscope (Nikon), and images captured by EZ-C1 Freeviewer software.

Results

Silibinin Feeding Reduces LUT Weight

Dietary silibinin feeding did not show any change in diet consumption and there was no considerable difference in body weight between silibinin-fed mice and respective positive

control group (data not shown). At necropsy, silibinin-fed groups showed lesser LUT weight compared to positive controls, though statistically not significant (data not shown). In non-transgenic mice, silibinin did not show any change in LUT weight (data not shown).

Silibinin Feeding Reduces Adenocarcinoma Incidence

H&E-stained sections were microscopically examined and classified as previously described (15) into (a) low grade PIN [LGPIN], (b) high grade PIN [HGPIN], (c) well differentiated [WD] adenocarcinoma, (d) moderately differentiated [MD] adenocarcinoma, and (e) poorly differentiated [PD] adenocarcinoma. Histopathological evaluation (Fig. 2A) revealed that at the time of sacrifice in 4-12 week groups, prostatic tissue in both positive control and silibinin-fed mice was at the PIN stage, with no evidence of adenocarcinoma in both groups. There was also no significant difference in the incidence of LGPIN and HGPIN between silibinin–fed mice and positive controls. While the type of PIN did not reveal much, the sections were re-analyzed for the pattern of PIN (Fig. 2A). It was observed that there was a higher incidence of diffused pattern of PIN with extensive involvement of most glands in the positive control group compared to a higher incidence of mixed pattern (diffused/focal) with involvement of some glands only in silibinin–fed group. Only 20% of silibinin-fed mice in 4-12 week group showed 100% involvement of glands whereas all animals in positive control group had 100% of their glands with PIN characteristics (Fig. 2A). In 12-20 week group, 90% of positive control mice showed PIN and 10% showed PD adenocarcinoma characteristics (Fig. 2B). In comparison, there was no evidence of adenocarcinoma with 100% of mice having PIN in silibinin-fed 12-20 week group. In 20-30 week group, none of the positive control mice showed PIN characteristics; on the other hand, there was 15% incidence of LGPIN and 44% incidence of HGPIN in silibinin-fed group (Fig. 2B). Also, there was 78% and 69% decrease in the incidence of WD and MD adenocarcinoma in 20-30 week silibinin–fed group compared to respective positive controls. Furthermore, a 53% reduction in the incidence of PD adenocarcinoma was observed in silibinin-fed group (Fig. 2B). At the time of sacrifice, mice in both silibinin–fed and positive control 30-45 week group showed large prostatic tumors. However, silibinin-fed group showed a 7% incidence of WD adenocarcinoma which was absent in positive controls that had a relatively higher, though statistically not significant, incidence of MD and PD adenocarcinoma (Fig. 2B).

Silibinin Feeding Reduces Tumor Grade

To assess severity of prostatic lesions, histological data were further analyzed for tumor grade. Tissues were graded according to the criteria, where (a) normal epithelium was assigned a score of 1.0; (b) LGPIN as 2.0; (c) HGPIN as 3.0; (d) WD adenocarcinoma as 4.0; (e) MD adenocarcinoma as 5.0; and (f) PD adenocarcinoma as 6.0. To generate a mean peak histological score, maximum histological score for individual prostate from each mouse was used to calculate a mean for that treatment group. There was no difference in tumor grade between 4-12 week positive control and silibinin-fed groups (Fig. 2C). In 12-20 week group, silibinin–fed mice had a slightly lower tumor grade compared to positive controls, though statistically insignificant; however, a significant reduction in the severity of lesions was observed in 20-30 week silibinin–fed mice showing lower tumor grade (mean peak score, 3.5; $P<0.001$) than positive controls (mean peak score, 4.9) (Fig. 2C). There was, however, no significant difference in tumor grade between 30-45 week positive control and silibinin-fed groups. The photomicrographs, representative of mean peak histological score of a treatment group, are shown in Fig. 2D.

Silibinin Feeding Reduces Proliferation Index

Quantification of PCNA staining showed a decrease in proliferation indices by 25% ($P<0.01$), 23% and 24% ($P<0.02$, for both) in 12-20, 20-30 and 30-45 week silibinin-fed groups of mice,

respectively; 4-12 week silibinin–fed group also decreased proliferation by 26%, but was not significant (Supplementary Figure 1A). These results suggest mostly non-stage specific *in vivo* anti-proliferative effect of silibinin during tumor growth and progression in the prostate of TRAMP mice. Regarding *in vivo* stage specific apoptotic response of silibinin feeding on prostate tumorigenesis in TRAMP mice, microscopic examination of tissue sections showed an increased number of TUNEL-positive cells in silibinin-fed groups (Supplementary Figure 1B); however, it was significant only in 12-20 week group where silibinin increased apoptotic cells by ~5-fold, $P<0.05$ (Supplementary Figure 1B).

Silibinin Modulates Cell Cycle Regulators

We also determined the stage specific effect of silibinin feeding on the expression of cell cycle regulators in the prostate of TRAMP mice. Western blots for Cdks, cyclins and Cdk inhibitors with densitometric data (adjusted with β-actin as loading control) are shown in Figure 3A-C. Here, it should be noted that membranes were stripped and reprobed for β-actin for each blot (data not shown). The expression levels of Cdk2, Cdk4 and Cdc2 were significantly increased ($P<0.001$) with progression in 20-30 and 30-45 week positive controls, while Cdk6 levels increased significantly ($P<0.001$) in 30-45 week positive controls. Silibinin feeding in 20-30 and 30-45 week groups strongly decreased Cdk2 expression by 84% and 45% ($P<0.001$, for both), respectively, but had no effect in other groups (Fig. 3A). Cdk4 expression was significantly decreased ($P<0.001$) by silibinin in all groups, except 30-45 week (Fig. 3A). Silibinin also decreased Cdk6 expression by 45% ($P<0.01$) and 84% ($P<0.001$) in 12-20 and 30-45 week groups, respectively, which was also evident in 20-30 week group though statistically not significant (Fig. 3A). Cdc2 expression was decreased by silibinin in all treatment groups with 99% ($P<0.02$), 92% ($P<0.02$), 70% ($P<0.001$) and 36% ($P<0.001$) decrease in 4-12, 12-20, 20-30 and 30-45 week groups, respectively (Fig. 3A). Regarding cyclins expression, levels of A and E were increased ($P<0.001$-$P<0.01$) with progression in 20-30 and 30-45 week positive controls, while B1 levels increased ($P<0.001$) after 12 weeks of age. Silibinin feeding significantly decreased cyclin A levels by 96% and 66% ($P<0.001$, for both) in 20-30 and 30-45 week groups, respectively (Fig. 3B). Levels of cyclin E were decreased by 95% ($P<0.001$) and 96% ($P<0.05$) in 12-20 and 20-30 week groups fed with silibinin, respectively (Fig. 3B). Cyclin B1 was significantly reduced in all silibinin groups showing 99% ($P<0.001$), 96% ($P<0.01$), 64% ($P<0.01$) and 24% ($P<0.001$) decrease in 4-12, 12-20, 20-30 and 30-45 week groups, respectively (Fig. 3B).

Regarding Cdk inhibitors, levels of p21 were significantly increased ($P<0.02$) in age groups higher than 4-12 weeks, but were not significantly different from each other. The levels of p21, though initially decreased by silibinin feeding in 4-12 and 12-20 week groups, significantly increased by 1.5-fold in 20-30 week group (Fig. 3C). The expression of p27 showed an increasing trend with progression but only became statistically significant in 30-45 week positive controls. The expression of p27 in 4-12 week silibinin–fed group was lower compared to respective positive controls with no difference in 12-20 week group; however, it was moderately increased in 20-30 and 30-45 week groups by silibinin feeding, though statistically not significant (Fig. 3C).

Silibinin Feeding Inhibits Angiogenesis in TRAMP Mice

The ability of localized carcinoma to further grow and metastasize is dependent upon its ability to recruit new vasculature *via* angiogenesis (18). With progression, vasculature invades epithelial layer of the ducts, and with higher expression of pro-angiogenic factors, leads to progression of neoplastic stage to invasive stages (19). Consistent with earlier reports, we observed stage-specific increase in intraductal MVD (1.7 ± 0.2 in 4-12 week group versus 43 ± 2 in 30-45 week group) with progression from PIN to WD adenocarcinoma and then to more aggressive tumors by IHC staining for PECAM-1/CD-31 expression (Fig. 4A). In prostatic

regions with normal histology, capillaries were distributed in stroma and did not enter epithelial layer of the ducts, while in PIN stages, inward growth of blood vessels was observed. With progression, number of blood vessels within PIN lesions increased, and as tumors advanced, blood vessels became larger in size and showed heterogeneous distribution. In 4-12 week group, silibinin did not affect intraductal MVD; however its treatment during 12-20 and 20-30 week groups significantly decreased MVD by 39-50% ($P<0.02$, for both). Silibinin feeding also decreased MVD in 30-45 weeks group, though statistically not significant. Next, we analyzed the potential molecular events targeted by silibinin for its antiangiogenic effect.

Silibinin Feeding Modulates the Expression of Angiogenesis Regulators

New vascular network developed during angiogenesis is preceded by an 'angiogenic switch' which involves the expression of pro-angiogenic factors including VEGF (20). HIF-1α, a transcription factor usually induced under hypoxic conditions, regulates the expression of pro-angiogenic factors such as VEGF and its receptors (20-23). Expression of VEGF was found to increase with tumor progression as determined by IHC (data not shown). Immunoblot analysis (Fig. 4A), indicated that VEGF expression was significantly increased ($P<0.01$-$P<0.05$) in 20-30 and 30-45 week positive controls, and decreased by 81% ($P<0.01$) and 32% ($P<0.001$) following silibinin treatment, respectively (Fig. 4A). Regarding the levels of VEGF receptors, no detectable expression of VEGF-R1 and VEGF-R2 was observed till 20 weeks of age in positive control group (Fig. 4B); however, VEGF-R1 expression was detected in 20-30 week positive control group which relatively decreased ($P<0.001$) in 30-45 week group. Conversely, expression of VEGF-R2 increased in 30-45 week group as compared to 20-30 week positive controls (Fig. 4B). Interestingly, the decreasing and increasing expression patterns for VEGF-R1 and VEGF-R2, respectively, with tumor progression, were reversed by silibinin treatment (Fig. 4B). IHC analysis for HIF-1α expression (Fig. 4C) indicated more of its cytoplasmic localization in lower age groups; however, with tumor progression, both nuclear and cytoplasmic localization was observed. While HIF-1α immunoreactivity scores were decreased by silibinin feeding in all treatment groups; the decrease was significant ($P<0.01$) in 20-30 week group. These results were corroborated by immunoblot analysis of prostatic tissue lysates which indicated that silibinin feeding significantly decreases HIF-1 expression by 40% ($P<0.01$), 45% ($P<0.02$), 43% ($P<0.05$) and 33% ($P<0.02$) in 4-12, 12-20, 20-30 and 30-45 week groups, respectively (Fig. 4C). HIF-1α is also known to induce inducible nitric oxide synthase (iNOS) that enhances tumor cell proliferation, increases the production of angiogenic factors, and facilitates neo-vascularization and invasion, and therefore is a potential target for inhibition of tumor angiogenesis (24). iNOS expression was also observed to increase during tumor progression in TRAMP mice as indicated by increased immunoreactivity scores from 1 to 2.9 in positive control group (Fig. 4D). Silibinin feeding significantly decreased ($P<0.05$) iNOS immunoreactivity scores in 20-30 week group. Immunoblot analysis also corroborated IHC results indicating higher expression of iNOS in positive control group after 20 weeks of age ($P<0.001$-$P<0.05$), which was significantly decreased (95%, $P<0.05$) by silibinin feeding (Fig. 4D). In 30-45 week group, though silibinin feeding slightly decreased iNOS levels (indicated by IHC and WB analyses), it was not significant (Fig. 4D). These results suggest that silibinin may target VEGF, VEGFR, HIF-1α and iNOS expression to inhibit angiogenesis and associated tumor progression in TRAMP mice.

Silibinin Feeding Inhibits Invasion, Migration and Metastasis in TRAMP Mice

The proteolytic disruption of extracellular matrix (ECM) by secreted or surface bound proteases, released either from tumor cells or stromal elements, facilitates the movement of newly formed vasculature and also results in invasion of tumor cells in to surrounding stroma (25-27). In TRAMP model, changes in the expression of proteases like matrix metalloproteinases (MMPs) and urokinase–type plasminogen (uPA), and an up regulation of their proteolytic activity are observed in prostate which have been associated with invasive,

migratory and metastatic potential of prostatic tumor (25). In our study, MMPs showed a stage-specific expression with prostate tumor progression in TRAMP mice where MMP-2, -3 and -9 were expressed in lower age groups, but their expressions were relatively significantly higher (P<0.001-P<0.01) in 20-30 and 30-45 week positive controls (Fig. 5A). Silibinin feeding decreased MMPs expression in all age groups, where it significantly decreased MMP-2, -3 and -9 levels by 78%, 75% and 100% (P<0.001-0.01) in 4-12 week group; MMP-2 and -3 by 80% and 67% (P<0.001, for both) in 12-20 week group; and MMP-2 and -9 by 84% and 74% (P<0.01, for both) in 20-30 week group, respectively (Fig. 5A). Silibinin feeding also significantly decreased MMP-2 expression by 21% (P<0.05) in 30-45 week group, but had no effect on MMP-3 and -9 levels in this group.

While protein levels of MMPs increased with prostate tumor progression in positive control group, the levels of tissue inhibitors of MMPs (TIMP) decreased at the same time (Fig. 5A). Silibinin feeding did not show any effect on TIMP-2 expression in 4-12 week group; however, it increased the expression of TIMP-2 in other treatment groups. Specifically, TIMP-2 levels were significantly increased (P<0.001) in 20-30 and 30-45 week silibinin-fed groups (Fig. 5A).

The receptor of uPA (uPAR) was moderately up-regulated with tumor progression (P<0.01) in 20-30 and 30-45 week positive controls, while silibinin feeding significantly decreased its expression by 71%, 66% and 52% (P<0.001-0.05) in 4-12, 12-20 and 20-30 week groups, respectively, without any considerable effect in 30-45 week group (Fig. 5B).

The expression of mesenchymal marker fibronectin was detected after 20 weeks of age in positive controls (Fig. 5B). While there was no expression of fibronectin till 30 weeks of age in silibinin-fed groups; silibinin significantly decreased its level by 95% (P<0.001) when fed to 30-45 week group (Fig. 5B). E-cadherin expression was detected in all groups fed with silibinin, as compared to a loss of E-cadherin expression with the progression of prostate tumorigenesis in positive controls (Fig. 5B). The expression of snail-1 was also significantly down regulated by silibinin feeding, suggesting that silibinin helped in retaining epithelial characteristics of prostatic tissue during stage-specific treatment regimens (Fig. 5B). The correlation of E-cadherin and snail expressions in prostatic tissue was also observed by IF localization studies (Fig. 5C). We observed that in PIN stage, E-cadherin was localized on the intercellular junctions; however, during prostate tumor progression, there was a loss in E-cadherin localization along with increased nuclear expression of snail-1 (Fig. 5C), indicating epithelial-mesenchymal transition (EMT) during tumor progression in the prostate of TRAMP mice.

The H& E stained tissue sections of lung, liver and kidney of positive controls and their respective silibinin-fed groups were microscopically analyzed for metastatic lesions, and their prostatic origin was confirmed by SV-40 T antigen staining. These results are summarized in Table 1. There were no metastatic lesions till 12 weeks of age in both the groups; however, with increasing age, more metastatic lesions were observed in positive control groups and the incidence of which was decreased in silibinin-fed mice.

Discussion

In the present study, we evaluated the stage-specific efficacy of silibinin treatment against PCa growth and progression in TRAMP mice. Silibinin was fed to TRAMP mice at different stages of prostate tumor development, and then its inhibitory effect on tumor growth, progression, invasion, migration and metastasis was evaluated together with the analyses of the molecules possibly involved with silibinin efficacy. Silibinin feeding to mice in 4-12 week group did not show any drastic effect; however, delayed the onset of neoplastic characteristics in some glands as observed by less percentage of glands involved in PIN compared to positive control group

showing 100% glands with PIN characteristics. This observation was supported by a moderate decrease in proliferation index, and at molecular level, by inhibitory effect on the expression of some of the cell cycle regulatory molecules. In 12-20 week group, it was anticipated that all mice would have developed PIN at the time of starting silibinin treatment for 8 weeks. Only a few mice showed PD adenocarcinoma characteristic in the prostate of positive control group, but there was no incidence of adenocarcinoma in silibinin-fed group; silibinin also arrested the progression at LGPIN stage. This anti- prostate tumor progression effect of silibinin was accompanied by a decrease in cell proliferation *via* modulation of cell cycle regulatory molecules as well as significantly increased (~5 fold) apoptotic index. The most significant effect on prostate tumor growth and progression was observed when silibinin was fed to mice in 20-30 week group. In this stage, silibinin significantly reduced both tumor grade as well as prostate adenocarcinoma incidence by slowing down tumor progression from PIN (pre-malignant) to adenocarcinoma (malignant) stages. Potential mechanisms for this anti-PCa effect of silibinin could be most likely a decrease in Cdk-cyclin kinase activity leading to an inhibition of cell cycle progression accompanied with decreased cell proliferation. The significance of the effect of silibinin on p21 expression, showing a marked decrease in 12-20 week group but an increase in 20-30 week group, remains to be studied. At the advanced stage, in 30-45 week group, when all the mice had different stages of adenocarcinoma, although silibinin did not show any considerable effect on MD and PD stages, it stopped the progression of WD stage in few mice. Together, based on these study outcomes, it could be concluded that silibinin would be most effective in inhibiting PCa progression when the disease is diagnosed at PIN stage.

Angiogenesis is an important event that facilitates tumor growth, progression and metastasis. VEGF is a critical endothelial cell mitogen that exhibits its effects *via* two affinity receptors VEGF-R1 and VEGF-R2; these receptors are also expressed in tumor cells (20,28). In TRAMP model, angiogenic switch corresponds to a series of molecular events that comprise of an early 'initiation event' associated with the expression of HIF-1α and VEGF-R1; and a later 'progression event' associated with the expression of VEGF-R2 which involves the progression of tumor from a differentiated stage to a poorly differentiated stage (20,29). In TRAMP mice, MVD has been observed to increase with prostate tumor grade (19). In the present study, silibinin inhibited angiogenesis as indicated by significant reduction in intraductal MVD along with decreased expression of VEGF. Furthermore, angiogenic switch was modified by silibinin feeding as indicated by altered expressions of VEGF-R1 and VEGF-R2. Additionally, silibinin also decreased the expression of HIF-1α and iNOS that induce angiogenesis. Overall, these antiangiogenic mechanisms of silibinin possibly played an important role in the observed suppression of PCa growth and progression.

The presence of MMPs and uPAR at early stages indicate that even during PIN development, tissue remodeling exists. In this regard, silibinin significantly inhibited the expression of MMPs and uPAR and increased the expression of TIMP, indicating a less invasive potential of the transformed cells. The ability of tumor cells to migrate and metastasize is attributed to a process known as EMT, which involves de-differentiation of glandular epithelial cells into a mesenchymal phenotype (30). While differentiation of epithelial cells into invasive migratory mesenchymal cells is a crucial step in embryonic development, it is potentially destructive if deregulated and acquired by tumor cells (26,30). The transcription factor snail-1 has been implicated in EMT; its expression and nuclear translocation leads to down regulation of epithelial genes such as desmoplakin, Muc-1, occludins and claudins and to induction of mesenchymal markers such as fibronectin, vimentin and MMPs (26,31). Snail-1 directly represses the transcription of E -cadherin which results in loss of E-cadherin and subsequent dissolution of E-cadherin-dependant intercellular junctions, loss of cell polarity, and tissue integrity (26,31). The mesenchymal characteristics thus acquired by tumor cells provide them with highly invasive and migratory potential to metastasize to different organs (26,30).

In view of above summarized reports, our finding that silibinin feeding resulted in the retention of epithelial characteristics indicating a modulatory effect on EMT, is highly significant. In 30-45 week group, the prostate pathology at the time of treatment had already advanced to adenocarcinoma stage. Silibinin feeding at this stage showed more differentiation in tumors compared to positive control group, which could be attributed to increased expression of E-cadherin and an emergence and retention of epithelial characteristics by silibinin treatment. A decreased expression of mesenchymal markers fibronectin and snail-1 also indicated that silibinin had an inhibitory effect on migratory potential of tumor cells. Consistent with this anticipation, a reduced incidence of metastasis was expected, and indeed, this was the case where silibinin treatment showed decreased incidence of distant metastasis in lung, liver and kidney.

In summary, the results of this stage-specific study indicate that, for most part, the tumor grade at the time of treatment determines the chemopreventive mechanisms for silibinin efficacy. During the early stages of prostate tumor development, silibinin mediates its chemopreventive effect mostly by inhibiting the progression at PIN stage *via* anti-proliferative cell cycle regulatory mechanisms. However, when the animals are burdened with higher stages of prostate tumor, silibinin feeding significantly decreases tumor grade *via* anti-proliferative and anti-angiogenesis mechanisms. The anti-angiogenesis together with inhibition of EMT *via* decreased expression of MMPs, snail-1 and fibronectin with an increase in E-cadherin level could account for the anti-metastatic effect of silibinin. Together, our findings suggest that silibinin could be effective at any stage of PCa diagnosis, and therefore, this non-toxic phytochemical has wide and potential implications to improve the morbidity and survival in PCa patients.

Supplementary Material

Refer to Web version on PubMed Central for supplementary material.

Acknowledgements

Grant support: This work was supported by NCI RO1 grant CA102514.

References

1. Stewart AB, Lwaleed BA, Douglas DA, Birch BR. Current drug therapy for prostate cancer: an overview. Curr Med Chem Anticancer Agents 2005;5:603–12. [PubMed: 16305482]
2. Brand TC, Canby-Hagino ED, Pratap Kumar A, et al. Chemoprevention of prostate cancer. Hematol Oncol Clin North Am 2006;20:831–43. [PubMed: 16861117]
3. Klein EA. Chemoprevention of prostate cancer. Annu Rev Med 2006;57:49–63. [PubMed: 16409136]
4. Singh RP, Agarwal R. Mechanisms of action of novel agents for prostate cancer chemoprevention. Endocr Relat Cancer 2006;13:751–78. [PubMed: 16954429]
5. Thompson IM. Chemoprevention of prostate cancer: agents and study designs. J Urol 2007;178:S9–S13. [PubMed: 17644117]
6. Mentor-Marcel R, Lamartiniere CA, Eltoum IE, Greenberg NM, Elgavish A. Genistein in the diet reduces the incidence of poorly differentiated prostatic adenocarcinoma in transgenic mice (TRAMP). Cancer Res 2001;61:6777–82. [PubMed: 11559550]
7. Raina K, Singh RP, Agarwal R, Agarwal C. Oral grape seed extract inhibits prostate tumor growth and progression in TRAMP mice. Cancer Res 2007;67:5976–82. [PubMed: 17575168]
8. Singh RP, Agarwal R. Prostate cancer chemoprevention by silibinin: bench to bedside. Mol Carcinog 2006;45:436–42. [PubMed: 16637061]
9. Gingrich JR, Barrios RJ, Kattan MW, et al. Androgen-independent prostate cancer progression in the TRAMP model. Cancer Res 1997;57:4687–91. [PubMed: 9354422]

10. Gingrich JR, Barrios RJ, Morton RA, et al. Metastatic prostate cancer in a transgenic mouse. Cancer Res 1996;56:4096–102. [PubMed: 8797572]
11. Gingrich JR, Greenberg NM. A transgenic mouse prostate cancer model. Toxicol Pathol 1996;24:502–4. [PubMed: 8864193]
12. Kaplan-Lefko PJ, Chen TM, Ittmann MM, et al. Pathobiology of autochthonous prostate cancer in a pre-clinical transgenic mouse model. Prostate 2003;55:219–37. [PubMed: 12692788]
13. Greenberg NM, DeMayo F, Finegold MJ, et al. Prostate cancer in a transgenic mouse. Proc Natl Acad Sci U S A 1995;92:3439–43. [PubMed: 7724580]
14. Greenberg NM, DeMayo FJ, Sheppard PC, et al. The rat probasin gene promoter directs hormonally and developmentally regulated expression of a heterologous gene specifically to the prostate in transgenic mice. Mol Endocrinol 1994;8:230–9. [PubMed: 8170479]
15. Raina K, Blouin MJ, Singh RP, et al. Dietary feeding of silibinin inhibits prostate tumor growth and progression in transgenic adenocarcinoma of the mouse prostate model. Cancer Res 2007;67:11083–91. [PubMed: 18006855]
16. Singh RP, Sharma G, Dhanalakshmi S, Agarwal C, Agarwal R. Suppression of advanced human prostate tumor growth in athymic mice by silibinin feeding is associated with reduced cell proliferation, increased apoptosis, and inhibition of angiogenesis. Cancer Epidemiol Biomarkers Prev 2003;12:933–9. [PubMed: 14504208]
17. Gu M, Dhanalakshmi S, Mohan S, Singh RP, Agarwal R. Silibinin inhibits ultraviolet B radiation-induced mitogenic and survival signaling, and associated biological responses in SKH-1 mouse skin. Carcinogenesis 2005;26:1404–13. [PubMed: 15831527]
18. Bhat TA, Singh RP. Tumor angiogenesis - A potential target in cancer chemoprevention. Food Chem Toxicol. 2007
19. Ozawa MG, Yao VJ, Chanthery YH, et al. Angiogenesis with pericyte abnormalities in a transgenic model of prostate carcinoma. Cancer 2005;104:2104–15. [PubMed: 16208706]
20. Huss WJ, Hanrahan CF, Barrios RJ, Simons JW, Greenberg NM. Angiogenesis and prostate cancer: identification of a molecular progression switch. Cancer Res 2001;61:2736–43. [PubMed: 11289156]
21. Forsythe JA, Jiang BH, Iyer NV, et al. Activation of vascular endothelial growth factor gene transcription by hypoxia-inducible factor 1. Mol Cell Biol 1996;16:4604–13. [PubMed: 8756616]
22. Marti HH, Risau W. Systemic hypoxia changes the organ-specific distribution of vascular endothelial growth factor and its receptors. Proc Natl Acad Sci U S A 1998;95:15809–14. [PubMed: 9861052]
23. Zhong H, De Marzo AM, Laughner E, et al. Overexpression of hypoxia-inducible factor 1alpha in common human cancers and their metastases. Cancer Res 1999;59:5830–5. [PubMed: 10582706]
24. Singh RP, Agarwal R. Inducible nitric oxide synthase-vascular endothelial growth factor axis: a potential target to inhibit tumor angiogenesis by dietary agents. Curr Cancer Drug Targets 2007;7:475–83. [PubMed: 17691907]
25. Bok RA, Hansell EJ, Nguyen TP, et al. Patterns of protease production during prostate cancer progression: proteomic evidence for cascades in a transgenic model. Prostate Cancer Prostatic Dis 2003;6:272–80. [PubMed: 14663466]
26. Przybylo JA, Radisky DC. Matrix metalloproteinase-induced epithelial-mesenchymal transition: tumor progression at Snail's pace. Int J Biochem Cell Biol 2007;39:1082–8. [PubMed: 17416542]
27. Radisky D, Muschler J, Bissell MJ. Order and disorder: the role of extracellular matrix in epithelial cancer. Cancer Invest 2002;20:139–53. [PubMed: 11852996]
28. Turner HE, Harris AL, Melmed S, Wass JA. Angiogenesis in endocrine tumors. Endocr Rev 2003;24:600–32. [PubMed: 14570746]
29. Isayeva T, Chanda D, Kallman L, Eltoum IE, Ponnazhagan S. Effects of sustained antiangiogenic therapy in multistage prostate cancer in TRAMP model. Cancer Res 2007;67:5789–97. [PubMed: 17575146]
30. Radisky DC. Epithelial-mesenchymal transition. J Cell Sci 2005;118:4325–6. [PubMed: 16179603]
31. Olmeda D, Jorda M, Peinado H, Fabra A, Cano A. Snail silencing effectively suppresses tumour growth and invasiveness. Oncogene 2007;26:1862–74. [PubMed: 17043660]

Abbreviations

PCa
prostate cancer

Sb
silibinin

TRAMP
transgenic adenocarcinoma of the mouse prostate

LUT
lower urogenital tract

PIN
prostatic intraepithelial neoplasia

LGPIN
low grade PIN

HGPIN
high grade PIN

WD
well differentiated

MD
moderately differentiated

PD
poorly differentiated

PCNA
proliferation cell nuclear antigen

TUNEL
terminal deoxynucleotidyl transferase dUTP nick-end labeling

Cdk
cyclin-dependent kinase

PECAM-1/CD-31
platelet endothelial cell adhesion molecule-1

VEGF
vascular endothelial growth factor

VEGF-R1
VEGF receptor-1

VEGF-R2
VEGF receptor-2

HIF-1α
hypoxia-inducible factor-1α

iNOS
inducible nitric oxide synthase

MVD microvessel density

uPA urokinase–type plasminogen

uPAR uPA receptor

MMP matrix metalloproteinase

TIMP tissue inhibitor of MMP

EMT epithelial-mesenchymal transition

IGF-1 insulin-like growth factor

DAB 3, 3′-diaminobenzidine

WB western blot

IHC immunohistochemical

IF immunofluorescence

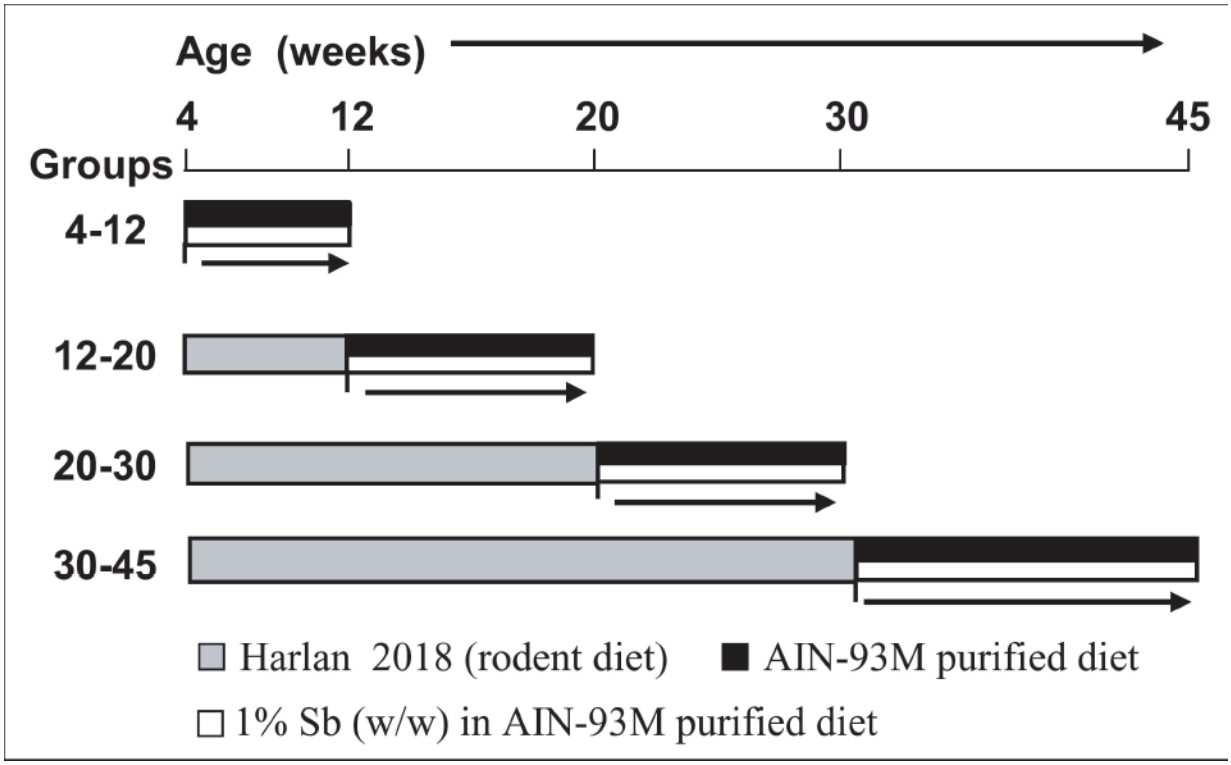

Fig. 1.

Experimental design to study the stage specific effect of dietary silibinin feeding on prostate tumor progression, invasion, migration and metastasis in TRAMP mice. Male TRAMP mice starting at 4, 12, 20 and 30 weeks of age were fed with control or 1% silibinin-supplemented [1% silibinin (w/w) in AIN-93M purified] diet and then sacrificed at 12, 20, 30 and 45 weeks of age, respectively. The different groups depending upon their study period were referred to as the 4-12, 12-20, 20-30 and 30-45 week groups, respectively. Sb, silibinin.

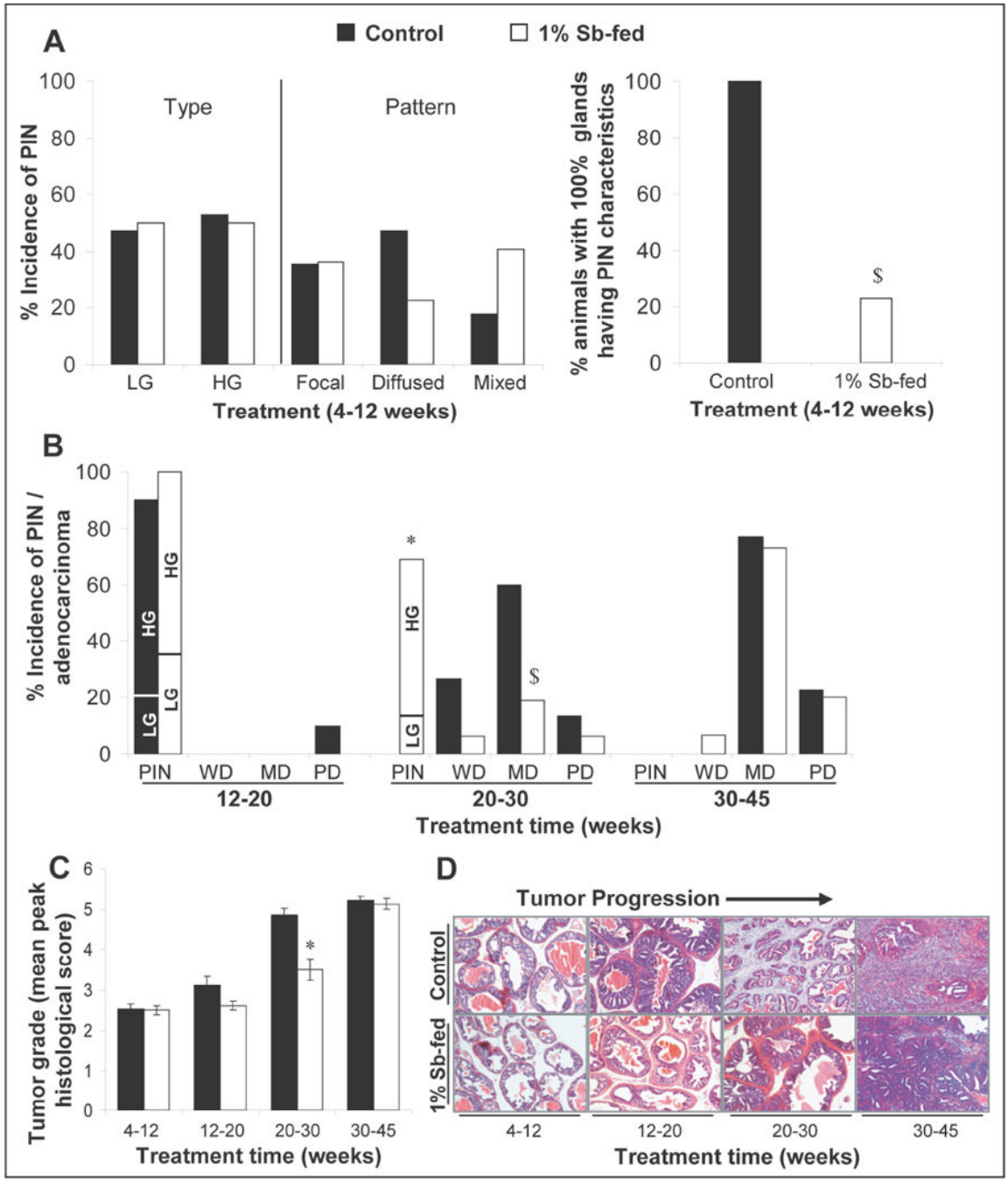

Fig. 2.

Silibinin feeding inhibits neoplastic progression of prostate in TRAMP mice at various stages. In the experiment detailed in Fig.1, at the time of necropsy dorsolateral prostate glands were harvested and histopathologically analyzed for the different stages of the neoplastic progression. (**A**) Effect of silibinin feeding on the incidence and pattern of PIN lesions in the 4-12 week group of TRAMP mice. (**B**) Effect of silibinin on the incidence of PIN/ adenocarcinoma of prostate in the 12-20, 20-30 and 30-45 week groups of TRAMP mice. Fisher's Exact test was used to compare incidence of PIN and adenocarcinoma in positive control versus silibinin-fed groups. *P* values <0.05 were considered significant. *, $P<0.001$; $, $P<0.05$. **(C)** Silibinin feeding reduces the severity of prostatic lesions (tumor grade) of TRAMP

prostate in a stage specific manner. Different stages of prostate tissues were graded as described in “Results”. The maximum histological score for the prostate lobe was used to calculate a mean for the treatment group. Data is presented as mean peak histological score and ± SEM (error bars) of each group. The difference between the positive controls versus the respective silibinin-fed group was analyzed by unpaired two-tailed Student’s *t*-test. *P* values <0.05 were considered significant. *, *P*<0.001. **(D)** The photomicrographs (×10 magnification) representative of the mean peak histological score of a treatment group show the H&E staining of the TRAMP prostate at different stages. Control, positive control (TRAMP mice); Sb, silibinin; PIN, prostate intraepithelial neoplasia; LG, low grade PIN; HG, high grade PIN; WD, well differentiated adenocarcinoma; MD, moderately differentiated adenocarcinoma; PD, poorly differentiated adenocarcinoma.

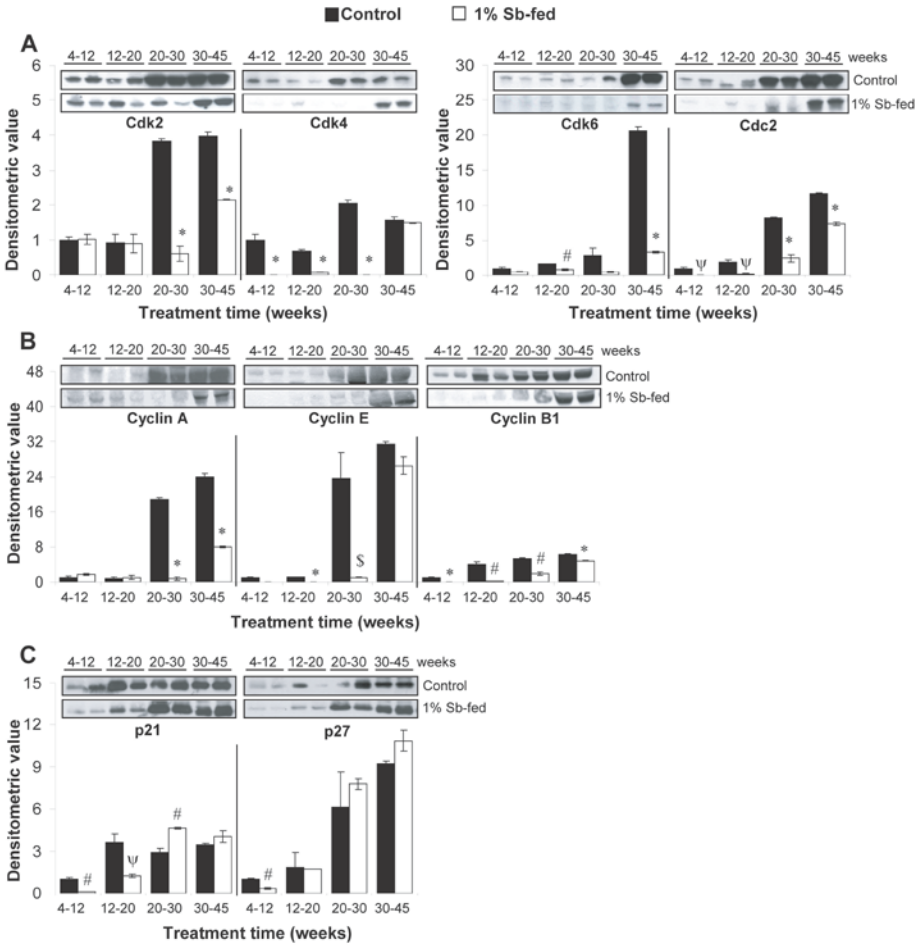

Fig. 3.

Stage specific effect of dietary feeding of silibinin on cell cycle regulatory molecules in the TRAMP prostate. **(A-C)** Silibinin feeding alters the expression levels of cell cycle regulatory molecules in the prostate of TRAMP mice in a stage specific manner. Randomly, four prostate tissue samples from individual mice were selected from each group for WB analyses detailed in "Materials and Methods". Reactive protein bands for the expression of Cdk2, Cdk4, Cdk6, Cdc2, cyclin A, cyclin E, cyclin B1, Cip1/p21 and Kip1/p27 were visualized by enhanced chemiluminescence detection system, and membranes were stripped and probed with β-actin as loading control. Densitometric analysis of band intensity for each protein was adjusted with β-actin (blots not shown). The results were reported as mean and ± SEM (error bars) of the four bands from individual mouse prostate in each group based on the relative densities compared to the 4-12 positive control group. Representative blots of two prostate samples from each group are shown. Difference among the positive control groups was determined by one-way ANOVA followed by Tukey-test for multiple comparisons and values are mentioned only in the 'Results section'. The difference between the positive controls versus the respective silibinin-fed group was analyzed by unpaired two-tailed Student's *t*-test. *P* values <0.05 were considered significant. *, $P<0.001$; #, $P<0.01$; ψ $P<0.02$, $, $P<0.05$. Control, positive control (TRAMP mice); Sb, silibinin; PCNA, proliferation cell nuclear antigen; Cdk, cyclin-dependent kinase.

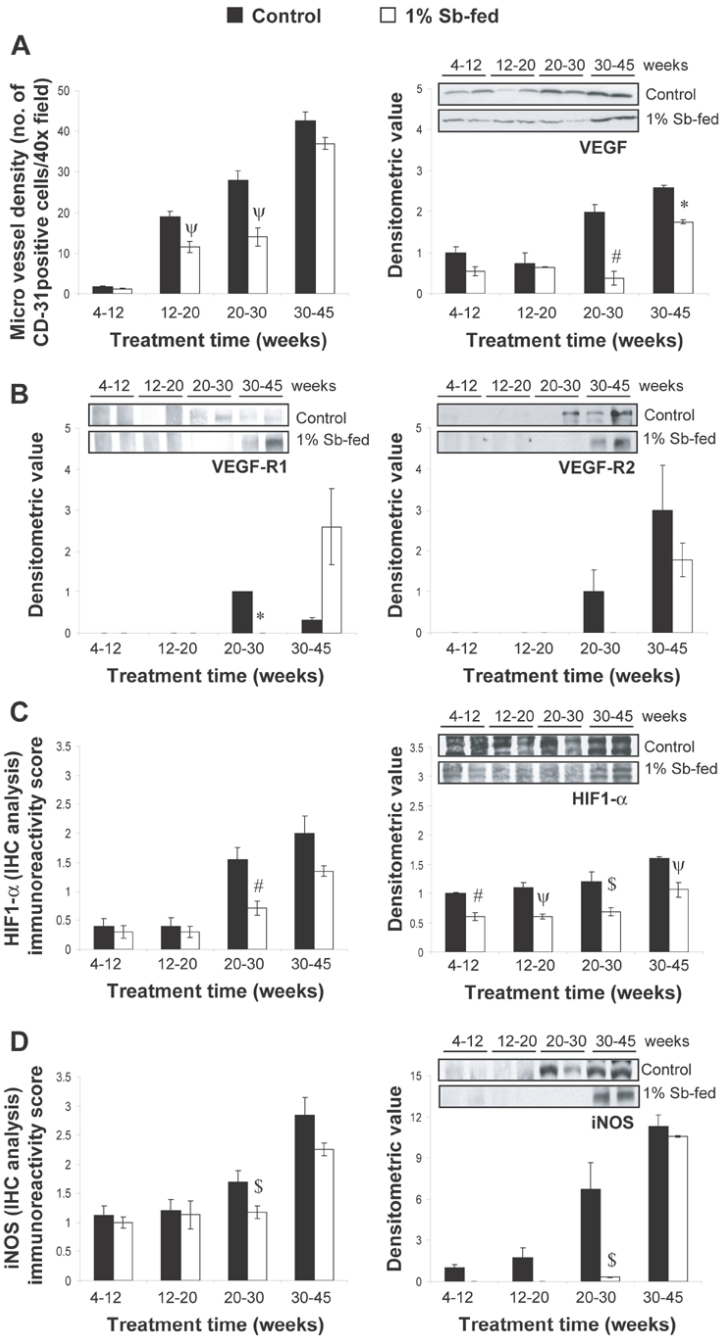

Fig. 4.

Stage specific effect of silibinin feeding on angiogenesis and pro-angiogenic markers in TRAMP prostate. **(A, left)** Effect of Silibinin feeding on intraductal MVD as inferred by IHC staining for the expression of PECAM-1/CD-31. IHC staining was based on DAB staining as detailed in “Materials and Methods”. Quantification of PECAM-1/CD-31-positive cells for determination of MVD is shown as mean and ± SEM (error bars) in each group. MVD was calculated as the number of positive cells × 100 / total number of cells counted under ×40 magnifications in 5 selected areas in each sample. **(A, right)** Stage specific effect of silibinin feeding on VEGF expression in TRAMP mice prostate as determined by WB analysis. **(B)** Stage specific effect of silibinin feeding on the expression levels of VEGF-R1 and VEGF-R2

in TRAMP mice prostate as determined by WB analysis. **(C-D)** Stage specific effect of silibinin feeding on the expression levels of HIF-1α and iNOS in TRAMP mice prostate as determined by IHC/WB analysis. Randomly, four prostate tissue samples from individual mice were selected from each group for WB analysis as detailed in "Materials and Methods". Reactive protein bands were visualized by enhanced chemiluminescence detection system, and membrane were stripped and probed with β-actin as loading control. Densitometric analysis of band intensity for each protein was adjusted with β-actin (blots not shown). The results were reported as mean and ± SEM (error bars) of the four bands from individual mouse prostate in each group based on the relative densities compared to the 4-12 positive control group. Representative blots of two prostate samples from each group are shown. Difference between the positive control groups was determined by one-way ANOVA followed by Tukey-test for multiple comparisons, and values are mentioned only in the "Results section". The difference between the positive controls versus the respective silibinin-fed group was analyzed by unpaired two-tailed Student's *t*-test. *P* values <0.05 were considered significant. *, $P<0.001$; #, $P<0.01$; ψ $P<0.02$, $, $P<0.05$. Control, positive control (TRAMP mice); Sb, silibinin; MVD, microvessel density; platelet endothelial cell adhesion molecule-1 (PECAM-1/CD-31); VEGF, vascular endothelial growth factor; VEGF-R1, VEGF receptor-1; VEGF-R2, VEGF receptor-2; HIF-1α , hypoxia-inducible factor-1α; iNOS, inducible nitric oxide synthase; WB, western blot; IHC, immunohistochemical.

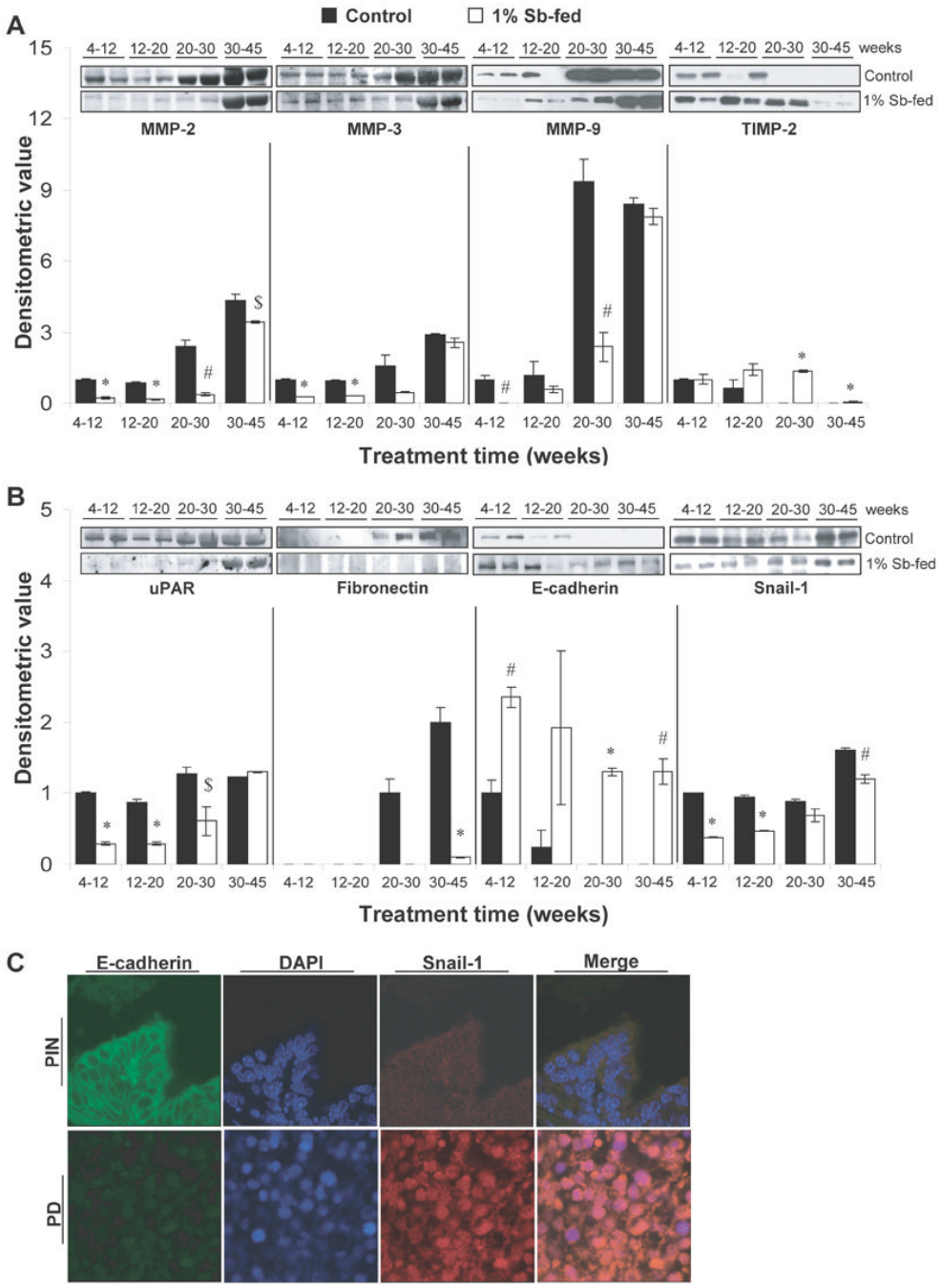

Fig. 5.

Stage specific effect of silibinin feeding on prostate tumor invasion, migration and epithelial mesenchymal transition in TRAMP prostate. **(A-B)** Reactive protein bands for the expression of MMP-2, 3, 9; TIMP-2; uPAR; fibronectin, E-cadherin and snail-1 were visualized by enhanced chemiluminescence detection system. Randomly, four prostate tissue samples from individual mice were selected from each group for WB analysis as detailed in "Materials and Methods". Reactive protein bands were visualized by enhanced chemiluminescence detection system, and membrane were stripped and probed with β-actin as loading control. Densitometric analysis of band intensity for each protein was adjusted with β-actin (blots not shown). The results were reported as mean and ± SEM (error bars) of the four bands from individual mouse

prostate in each group based on the relative densities compared to the 4-12 positive control group. Representative blots of two prostate samples from each group are shown. Difference between the positive control groups was determined by one-way ANOVA followed by Tukey-test for multiple comparisons, and values are mentioned only in the 'Results section'. The difference between the positive controls versus the respective silibinin-fed group was analyzed by unpaired two-tailed Student's *t*-test. *P* values <0.05 were considered significant. *, $P<0.001$; #, $P<0.01$; $, $P<0.05$. Control, positive control (TRAMP mice); Sb, silibinin; MMP, matrix metalloproteinase; TIMP, tissue inhibitor of MMP; uPAR, urokinase–type plasminogen; receptor. (C) IF localization studies to determine the correlation of E-cadherin and snail expression in prostatic tissue. Prostatic tissue was double stained for E-cadherin (green) and snail-1 (red) expression. Nuclear staining was done with DAPI (blue). Photomicrographs (×100 magnification). IF, Immunofluorescence; PIN, prostate intraepithelial neoplasia; PD, poorly differentiated adenocarcinoma.

Table 1

Stage specific effect of silibinin feeding on prostate tumor metastasis to lungs, liver and kidney in TRAMP mice

Treatment time (weeks)	% incidence of metastatic lesions					
	Lung		Liver		Kidney	
	Control	1% Sb-fed	Control	1% Sb-fed	Control	1% Sb-fed
4-12	0	0	0	0	0	0
12-20	10	0	6	0	6	0
20-30	78	24*	34	14	50	10#
30-45	100	72	75	57	88	64

In the experiment detailed in Fig.1, at the time of necropsy any evidence of gross metastatic lesions in non-target organs was noted. H& E stained tissue sections of lung, liver and kidney of positive controls and their respective silibinin-fed groups were microscopically analyzed for metastatic lesions. Values are shown as percent of mice having metastatic lesions in particular organ for each group. Fisher's Exact test was used to compare the incidence of metastatic lesions in positive control versus silibinin-fed groups. The numbers of animals in 4-12, 12-20, 20-30 and 30-45 week groups were 17, 20, 15 and 22 in the positive control groups; and 22, 18, 16 and 15 in the 1% Sb-fed groups, respectively. *P* values <0.05 were considered significant.

*$P<0.001$;

#$P<0.01$.

Control, positive control (TRAMP mice); Sb, silibinin.